

## Electronic Supplementary Information

### Piezoelectric Nanogenerators Synthesized Using $\text{KNbO}_3$

#### Nanowires with Various Crystal Structures

Mi-Ri Joung,<sup>a</sup> HaiBo Xu,<sup>a</sup> In-Tae Seo,<sup>a</sup> Dae-Hyeon Kim,<sup>a</sup> Joon Hur,<sup>b</sup> Sahn Nahm,<sup>\*a,b,c</sup> Chong-Yun Kang,<sup>b,c</sup> Seok-Jin Yoon<sup>c</sup> and Hyun-Min Park<sup>d</sup>

<sup>a</sup>Department of Materials Science and Engineering, Korea University, Seoul 136-713, Republic of Korea

<sup>b</sup>Department of Information Technology-Nano Science, Korea University-Korea Institute of Science and Technology School, Korea University, Seoul 136-713, Republic of Korea

<sup>c</sup>Electronic Materials Center, Korea Institute of Science and Technology, Seoul 136-791, Republic of Korea

<sup>d</sup>Center for Nanomaterials Characterization, Korea Research Institute of Standards and Science, Daejeon 305-340, Republic of Korea

\*Tel: +82-2-3290-3279, Fax: +82-2-928-3584

E-mail address: [snahm@korea.ac.kr](mailto:snahm@korea.ac.kr)

## **I. Calculation of strain developed in the K-P composite**

### **1. Determine the strain neutral line**

In order to calculate the strain developed in the K-P composite, the strain neutral line was determined using the following equation:

$$Y_{PI}t_1y_1 + Y_Ct_2y_2 + Y_{PI}t_3y_3 + Y_{PET}t_4y_4 = 0 \quad (1),$$

where  $Y_{PI}$ ,  $Y_C$ , and  $Y_{PET}$  are Young's modulus of PI, the K-P composite, and PET, respectively,  $t_1$ ,  $t_2$ ,  $t_3$ , and  $t_4$  represent the thickness of the top PI layer, the K-P composite, and the bottom PI and PET layers, respectively, and  $y_1$ ,  $y_2$ ,  $y_3$ , and  $y_4$  denote the distance between the strain neutral line and the center of the top PI layer, the K-P composite, the bottom PI and PET layers, respectively.  $Y_{PI}$  and  $Y_{PET}$  are known to be 2.5 GPa and 2.7 GPa, respectively.  $Y_C$  was calculated to be 0.7 GPa under iso-stress conditions by using Young's modulus of KNbO<sub>3</sub> (91 GPa) and PDMS (0.615 GPa) and the volume fraction of KNbO<sub>3</sub> (0.06) and PDMS (0.94).

### **2. Calculation of strain developed in the K-P composite ( $\epsilon_l$ )**

The strain developed in the K-P composite was calculated using the following equation:

$$\epsilon_l = \frac{y_2}{r} = 2y_2 \times \frac{h}{\left(\frac{d}{2}\right)^2 + h^2} \quad (2)$$

where  $r$ ,  $d$ , and  $h$  represent the arc radius of the strain neutral plane, the device-length, and the arc height, respectively.

### **3. Calculation of strain developed in the K-P composite along the film direction ( $\epsilon_t$ )**

The strain calculated using equation (2) ( $\epsilon_l$ ) is the same as the strain developed in the K-P composite parallel to the interface between the K-P composite and the Au electrode. The strain developed in the K-P composite along the film direction ( $\epsilon_t$ ) was perpendicular to  $\epsilon_l$ ,

indicating that  $\varepsilon_t$  could be obtained using the Poisson's ratio of PDMS (0.5).<sup>1</sup> Therefore, the strain along the film direction ( $\varepsilon_l$ ) was  $0.5 \times \varepsilon_t$ . However, since the Young's modulus of PDMS (0.615 GPa) is much smaller than that of the KN nanowires (91 GPa),<sup>2</sup> the strain developed in the KN nanowires could be smaller than the strain developed in the K-P composite.

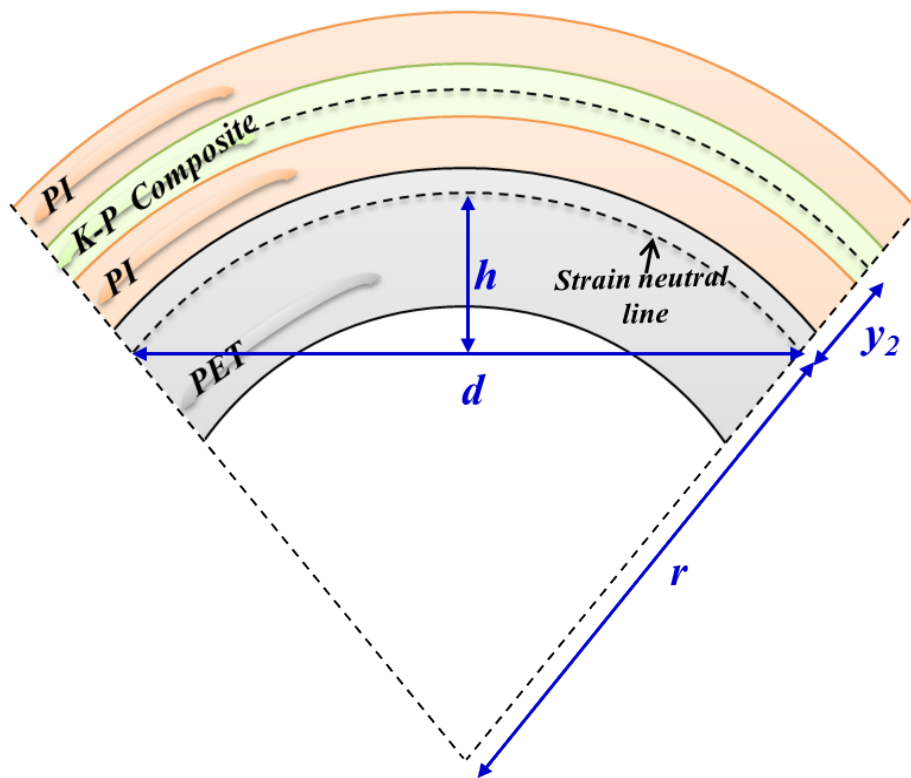


**Figure S1.** Schematic diagram of NG: PI-Au/K-P composite/Au-PI/PET.

## **II. Determination of Crystal Structure of KN Nanowires**

Rietveld analysis was conducted on the XRD patterns of the tetragonal and orthorhombic KN nanowires, as shown in Figures S2 and S3, respectively. The lattice parameters of the tetragonal and orthorhombic KN nanowires were easily evaluated using the full-pattern refinement method carried out by the Full prof program (Rodriguez-Carvajal, 2007); the lattice parameters are listed in Table S1. The profile matching of the XRD pattern of the PPB KN nanowires was carried out to identify the precise crystal structure of these nanowires, as shown in Figure S4. The unit cell of the PPB KN nanowire can be explained by the mixture of a tetragonal phase with the space group  $P4mm$  and an orthorhombic phase with the space group  $Amm2$ . The refined lattice parameters were  $a = 4.0074(1) \text{ \AA}$  and  $c = 4.0401(3) \text{ \AA}$  for the tetragonal phase and  $a = 3.9875(3) \text{ \AA}$ ,  $b = 5.7039(9) \text{ \AA}$ , and  $c = 5.7120(9) \text{ \AA}$  for the orthorhombic phase. The final refinement pattern is shown in Figure S4.

**Table S1.** Lattice parameters of KN nanowires with various structures.

<b>Lattice parameters</b>	
<b>(a) Tetragonal KN nanowires</b>	<b><math>a = 4.0046(2)\text{\AA}</math>, <math>c = 4.0415(2)\text{\AA}</math></b>
<b>(b) Orthorhombic KN nanowires</b>	<b><math>a = 3.9932(2)\text{\AA}</math>, <math>b = 5.6978(6)\text{\AA}</math>, <math>c = 5.7027(6)\text{\AA}</math></b>
<b>(c) PPB KN nanowires</b>	<b><math>a = 4.0074(1)\text{\AA}</math>, <math>c = 4.0401(3)\text{\AA}</math> <math>a = 3.9875(3)\text{\AA}</math>, <math>b = 5.7039(9)\text{\AA}</math>, <math>c = 5.7120(9)\text{\AA}</math></b>

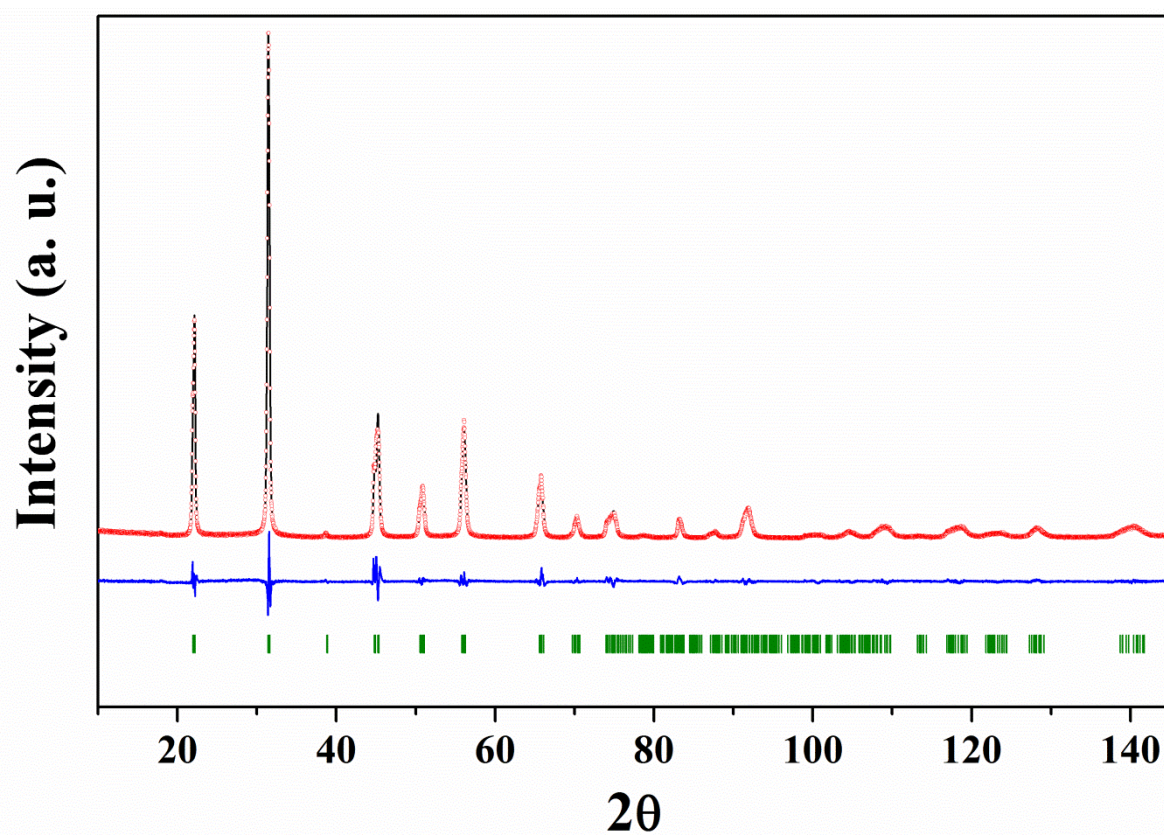


**Figure S2.** Full XRD pattern of the tetragonal KN nanowires. The refined model is a tetragonal unit cell with the space group of  $P4mm$ . The observed data are shown as open circles, and the calculated data are denoted by the solid line overlying them. The lower curve shows the difference between the observed and calculated diffraction patterns, and the short vertical bars are Bragg reflection markers. The profile R factor ( $R_p$ ) and weighted profile R factor ( $R_{wp}$ ) are 8.75% and 11.7%, respectively.

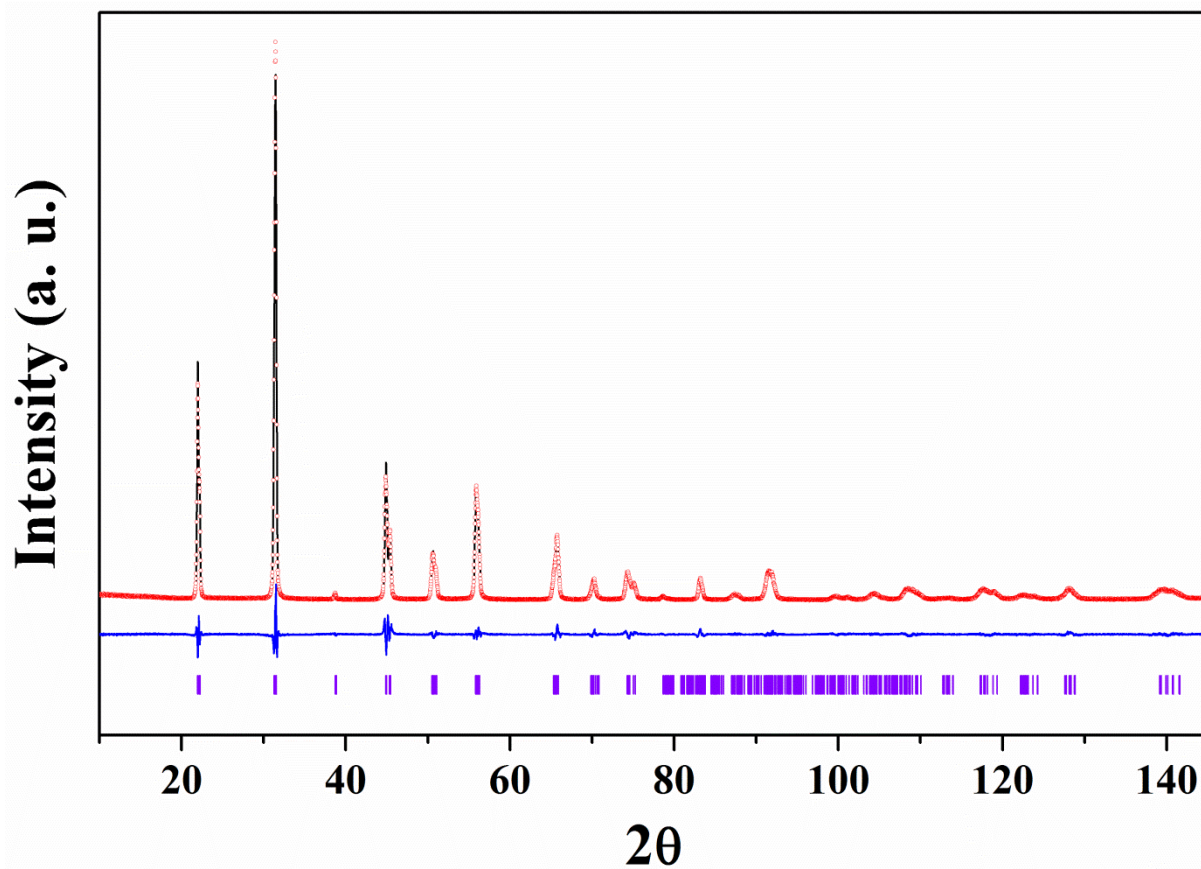


**Figure S3.** Full XRD pattern of the orthorhombic KN nanowires. The refined model is an orthorhombic unit cell with a space group of *Amm*2. The observed data are shown as open circles, and the calculated data are denoted by the solid line overlying them. The lower curve shows the difference between the observed and calculated diffraction patterns, and the short vertical bars are Bragg reflection markers.  $R_p$  and  $R_{wp}$  are 8.71% and 11.6%, respectively.

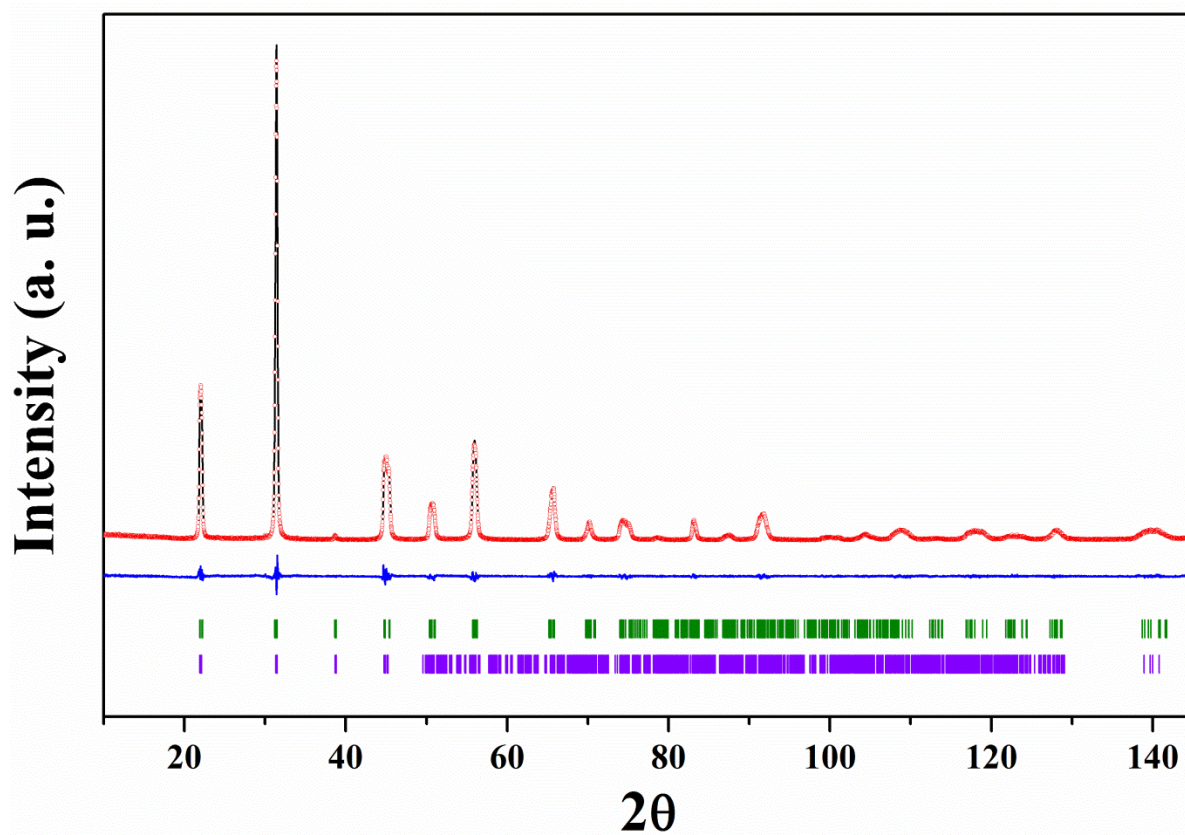


**Figure S4.** Full XRD pattern of the PPB KN nanowires. The refined models contain tetragonal and orthorhombic phases of KN. The observed data are shown as open circles, and the calculated data are denoted by the solid line overlying them. The lower curve shows the difference between the observed and calculated diffraction patterns, and the short vertical bars are Bragg reflection markers.  $R_p$  and  $R_{wp}$  are 5.94% and 8.85%, respectively.



**III. Electrical output characteristics of NGs containing 0.7 g of KN nanowires measured along the reverse direction**

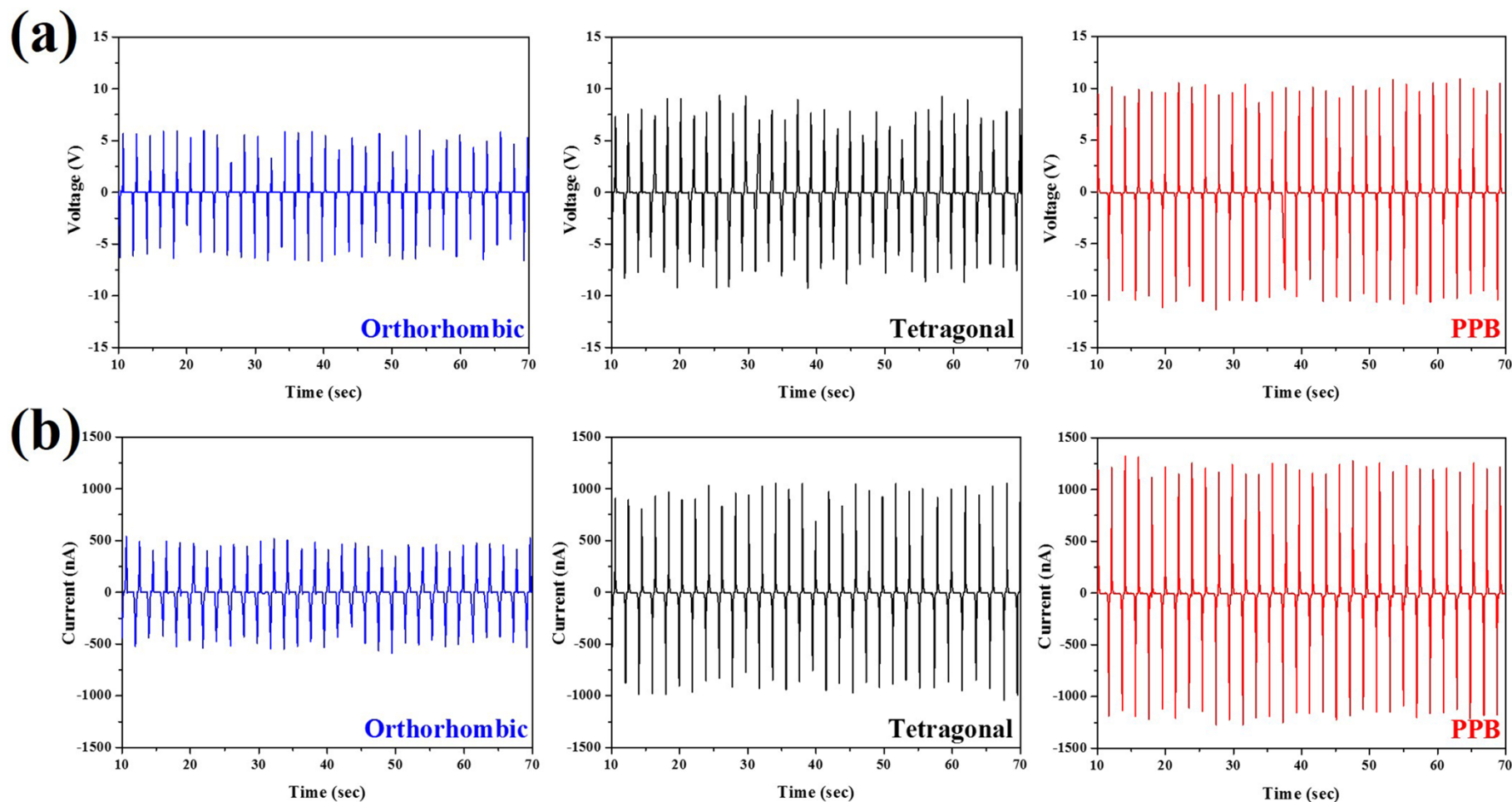


**Figure S5.** (a) Open-circuit voltage and (b) short-circuit current of NGs containing 0.7 g of KN nanowires having various structures, as measured along the reverse direction at a strain and strain rate of 2.1% and 2.2% s<sup>-1</sup>, respectively.

#### **IV. Electrical output characteristics of NGs containing 0.3 g of KN nanowires**

Figures S6(a) and (b) show the open-circuit voltage and short-circuit current of NGs containing 0.3 g of KN nanowires, as measured along the forward direction with a strain and strain rate of 2.1% and 2.2% s<sup>-1</sup>, respectively. These NGs showed a smaller output electrical energy than the NGs containing 0.7 g of KN nanowires. However, the variations of the output voltage and output current of these NGs with respect to the structure of the KN nanowires were similar to those of the NGs containing 0.7 g of KN nanowires. The maximum output voltage of 6 V and current of 0.6 μm were obtained from the NG containing PPB KN nanowires. Similar results were obtained when the output voltage and output current were measured along the reverse direction, as shown in Figures S7(a) and (b).

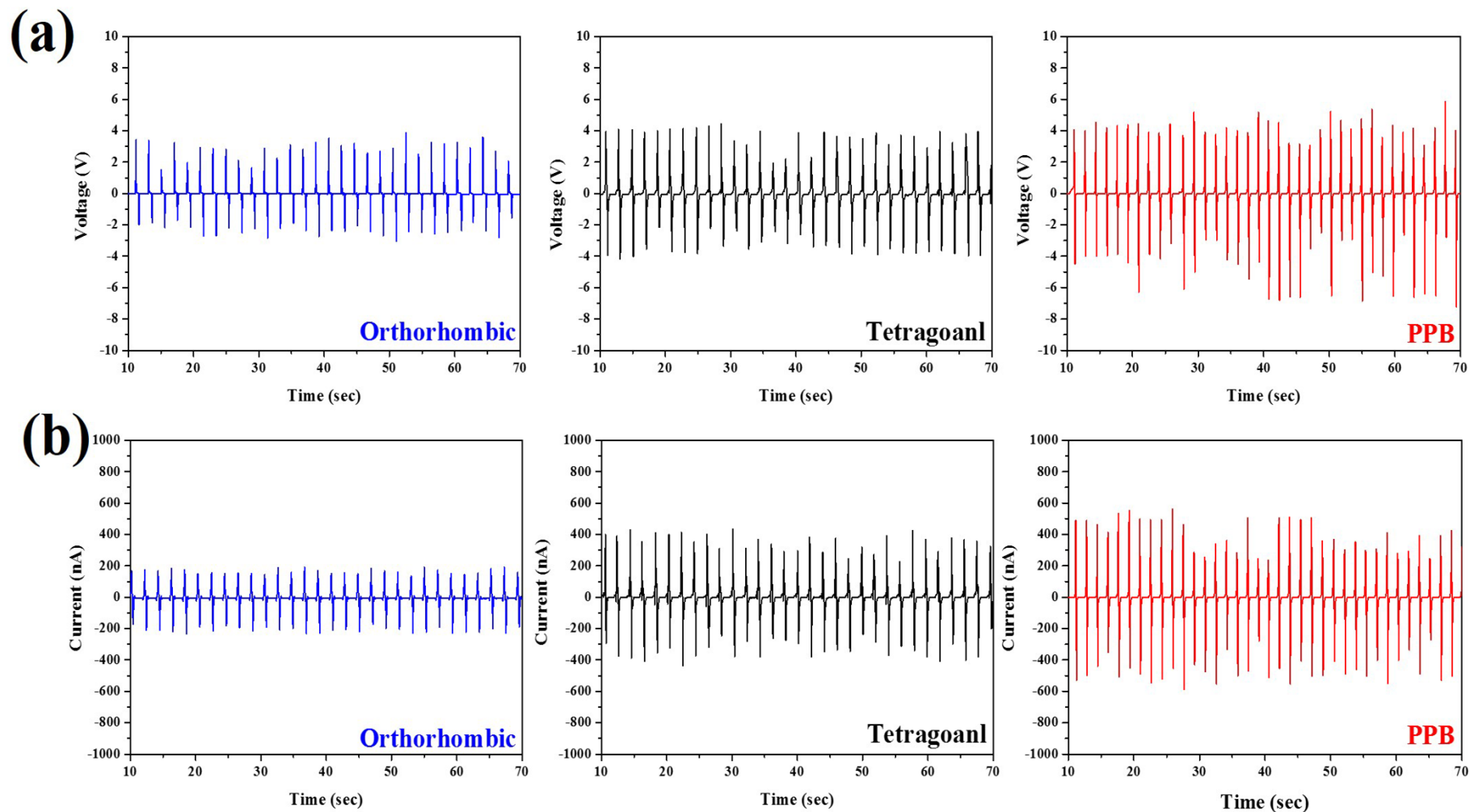


**Figure S6.** (a) Open-circuit voltage and (b) short-circuit current of NGs containing 0.3 g of KN nanowires having various structures, as measured along the forward direction at a strain and strain rate of 2.1% and  $2.2\% \text{ s}^{-1}$ , respectively.

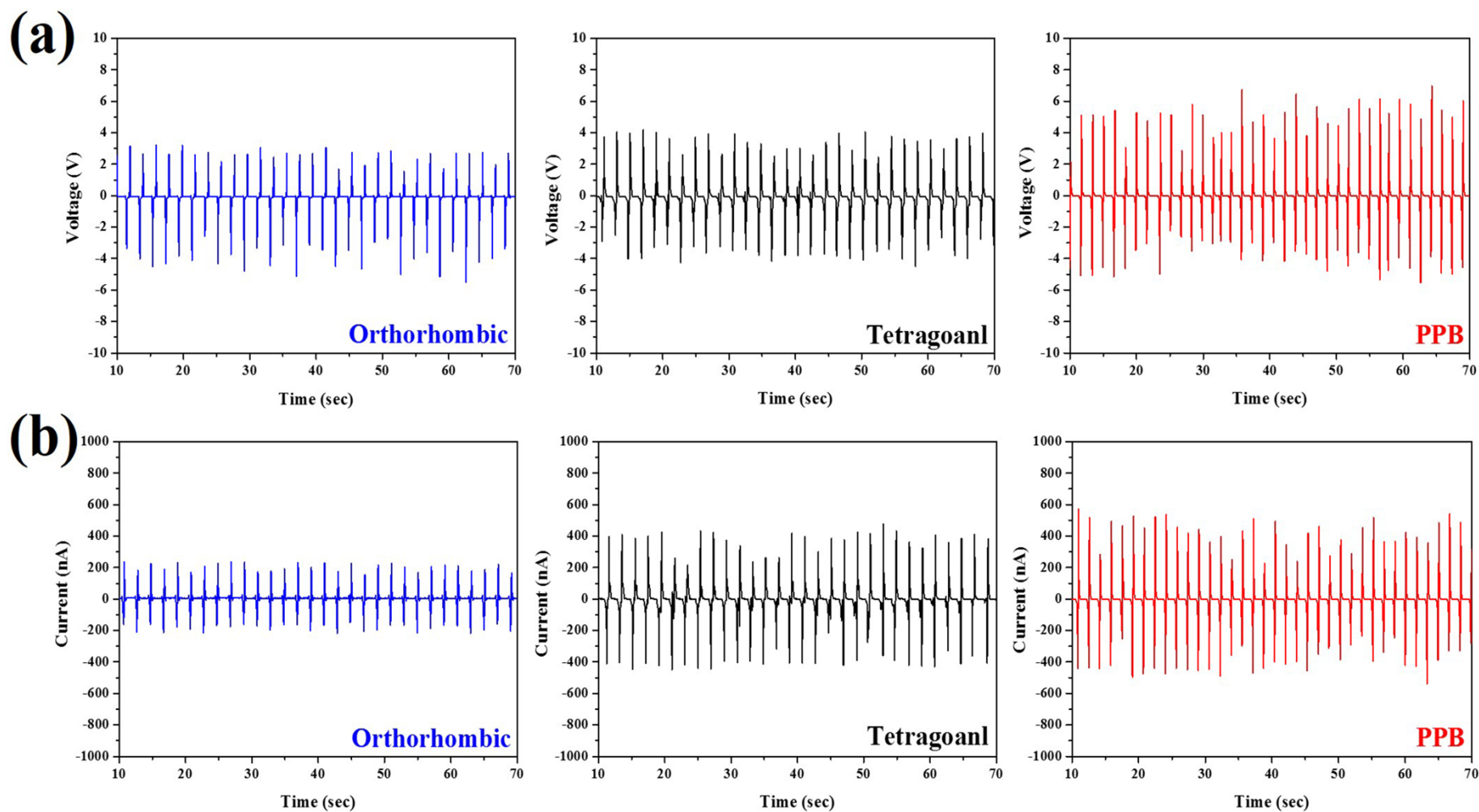


**Figure S7.** (a) Open-circuit voltage and (b) short-circuit current of NGs containing 0.3 g of KN nanowires having various structures, as measured along the reverse direction at a strain and strain rate of 2.1% and  $2.2\% \text{ s}^{-1}$ , respectively.

## **V. Calculation of output power and energy conversion efficiency**

We calculated the output power of the NGs by measuring the output voltages of the NGs using external loads. Figure S8 shows the electric circuit used for the measuring the output voltages of the NG using external loads, which were varied from 1.0 k $\Omega$  to 100 M $\Omega$ . Figures S9(a)-(c) show the output voltages obtained for a load of 1.0 M $\Omega$  for the NGs containing 0.7 g of the orthorhombic, tetragonal, and PPB KN nanowires, respectively; the strain was 2.1 % and the strain rate was 2.2 % s<sup>-1</sup>. The NG containing PPB KN nanowires showed a maximum output voltage (3.0 V). Similar output voltages were obtained when the measurement direction was the reversed, as shown in Figures S10(a)-(c). It is worth mentioning that the root mean square value of the measured peak voltage ( $V_{\text{rms}}$ ) was used to calculate the output currents and output powers of the NGs.

Figure S11(a) shows the variations in  $V_{\text{rms}}$ , the output current, and the output power of the NG containing orthorhombic KN nanowires for different external loads. The maximum output power (0.32  $\mu\text{W}$ ) was obtained at an external load of 1.0 M $\Omega$  for this NG. Similarly, the variations in  $V_{\text{rms}}$ , the output current, and the output power of the NG containing tetragonal KN nanowires are shown in Figure S11(b). This NG exhibited a maximum output power of 0.85  $\mu\text{W}$  at an external load of 1.0 M $\Omega$ . Finally, the variations in  $V_{\text{rms}}$ , the output current, and the output power of the NG containing PPB KN nanowires for different external loads are shown in Figure S11(c). The maximum output power for this NG, which was 4.5  $\mu\text{W}$ , was obtained at an external load of 1.0 M $\Omega$ . Therefore, the NG containing PPB KN nanowires exhibited the maximum output power. The output power of each NG is listed in Table S2.

The input mechanical energy can be calculated using the following equation:<sup>3,4</sup>

$$W_m = \frac{1}{8}\pi D^2 E \varepsilon^2 L_0$$

where  $D$  is the diameter of the nanowire,  $L_0$  is the length of the nanowire,  $E$  is the Young's modulus of the nanowire, and  $\varepsilon$  is the strain developed in the nanowires. Moreover, the output electrical energy can be calculated using the following equation:

$$W_e = \int VI dt$$

where  $V$  is the output voltage and  $I$  is the output current. Therefore, the energy conversion

efficiency of the KN nanogenerator is  $W_e/W_m$ . Table S2 below shows the output power and energy conversion efficiency of the NGs consisting of tetragonal, orthorhombic, and PPB KN nanowires (0.7 g).

**Table S2.** Output powers and energy conversion efficiencies of NGs containing 0.7 g of tetragonal, orthorhombic, and PPB KN nanowires.

	<b>Output power (<math>\mu\text{W}</math>)</b>	<b>Energy conversion efficiency (%)</b>
<b>Tetragonal</b>	<b>0.85</b>	<b>0.20</b>
<b>Orthorhombic</b>	<b>0.32</b>	<b>0.04</b>
<b>PPB</b>	<b>4.5</b>	<b>0.93</b>

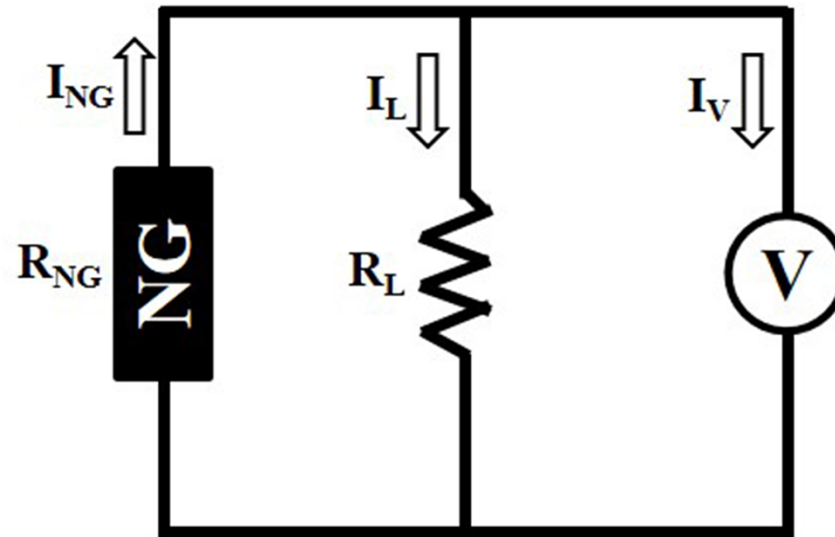


**Figure S8.** Electric circuit used to measure the output voltage of the NG using external load.

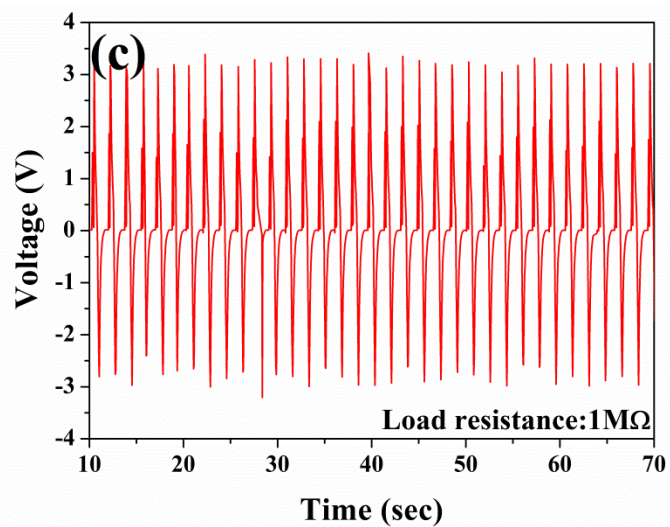
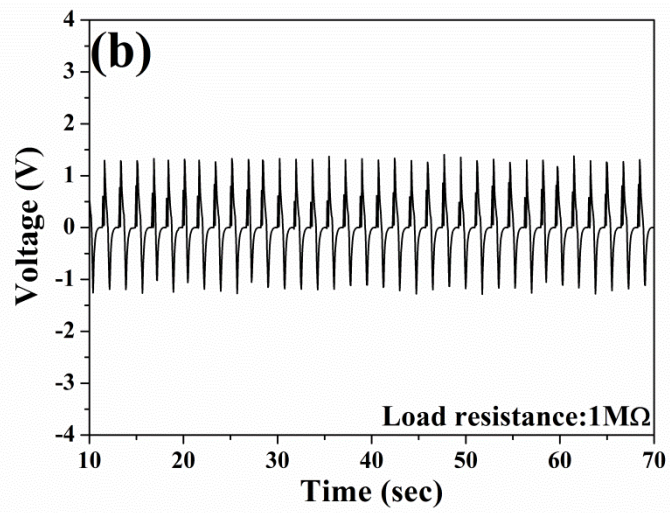
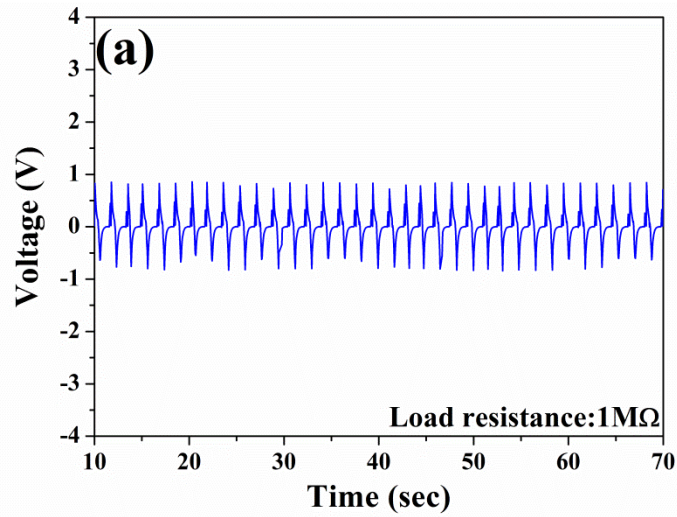


**Figure S9.** The output voltages obtained along the forward direction with the 1.0 M $\Omega$  external load and a strain of 2.1 % and a strain rate of 2.2 % s<sup>-1</sup> for the NGs containing 0.7 g of (a) orthorhombic, (b) tetragonal and (c) PPB KN nanowires.



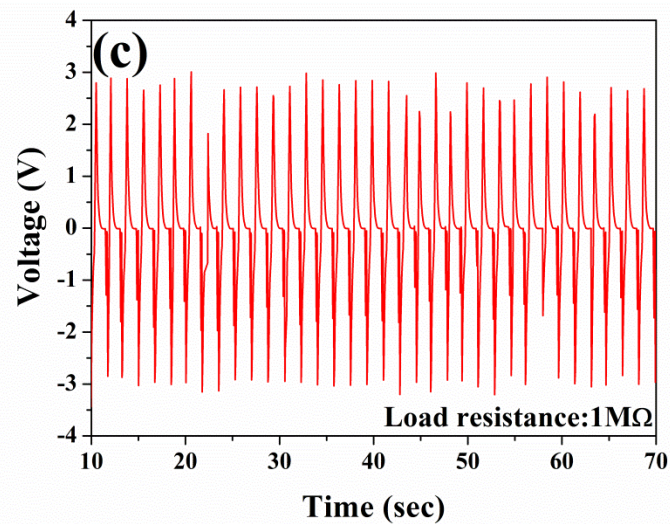
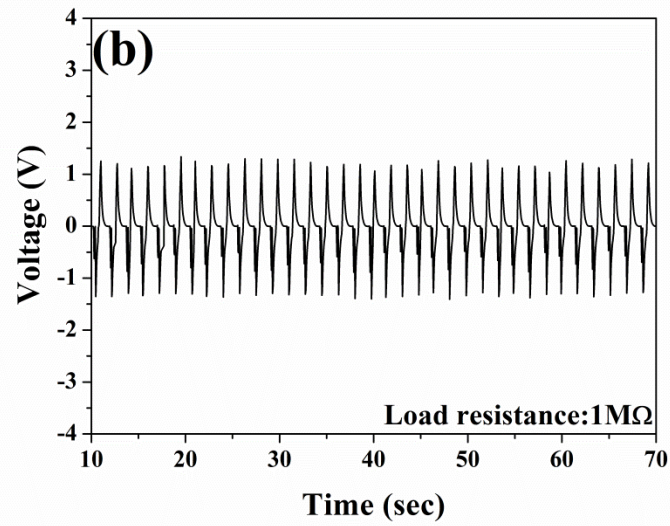
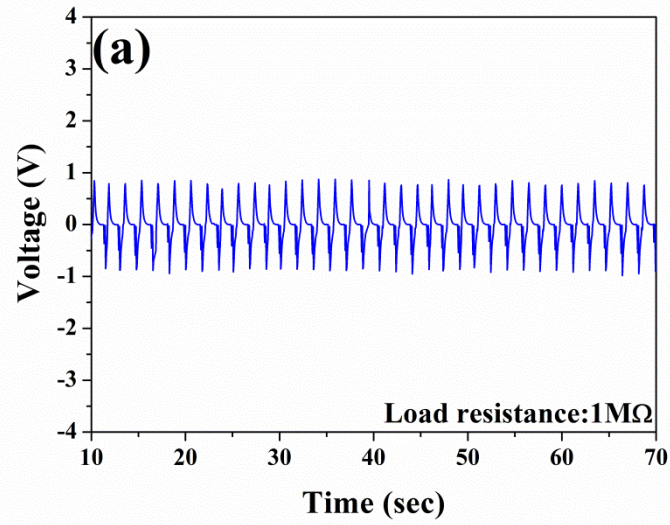


**Figure S10.** The output voltages obtained along the reverse direction with the  $1.0\text{ M}\Omega$  external load and a strain of  $2.1\%$  and a strain rate of  $2.2\% \text{ s}^{-1}$  for the NGs containing  $0.7\text{ g}$  of (a) orthorhombic, (b) tetragonal and (c) PPB KN nanowires.

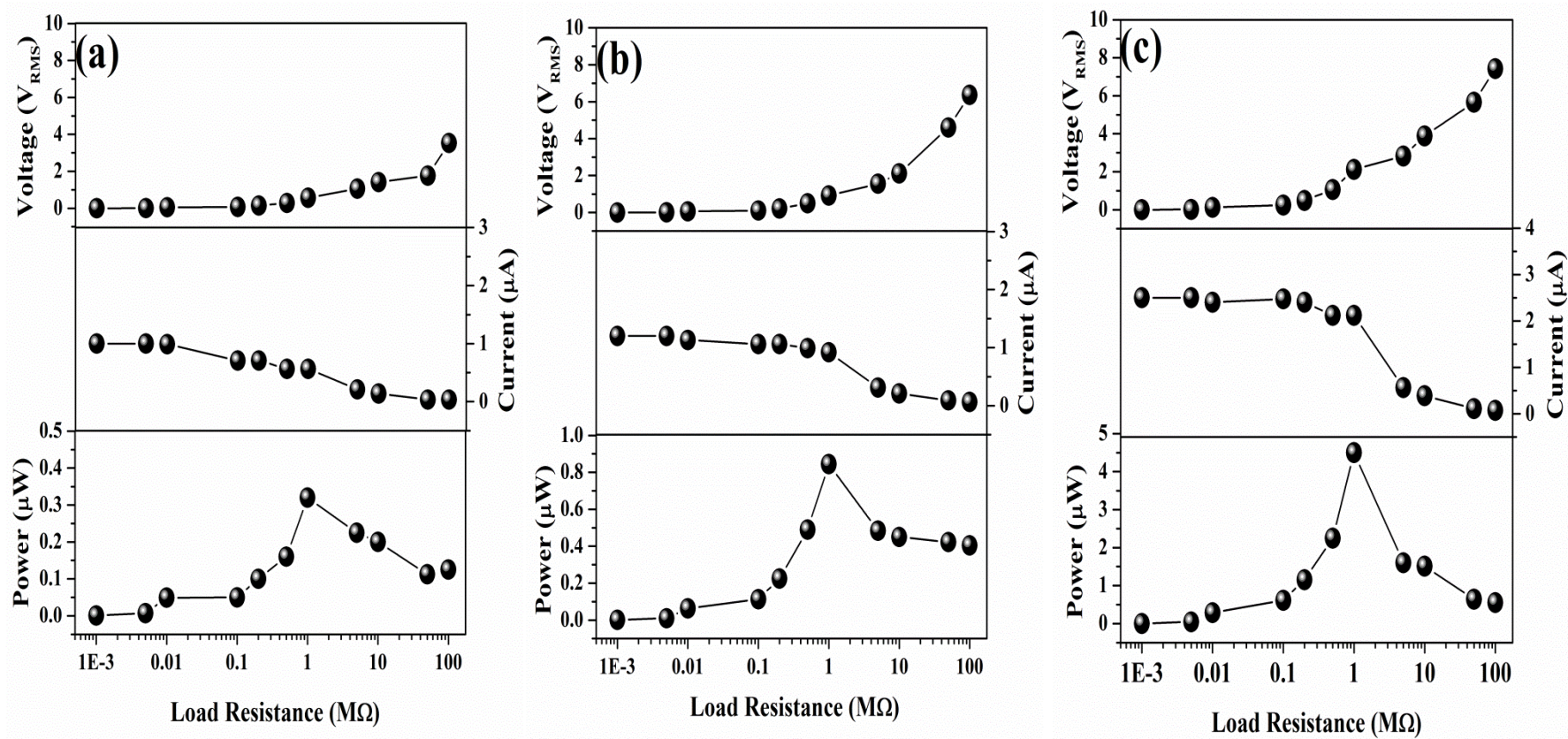


**Figure S11.** Variations of the  $V_{\text{rms}}$ , the output current and the output powers of the NG containing (a) orthorhombic, (b) tetragonal and (c) PPB KN nanowires.

## VI. Electrical output characteristics of the PDMS NG

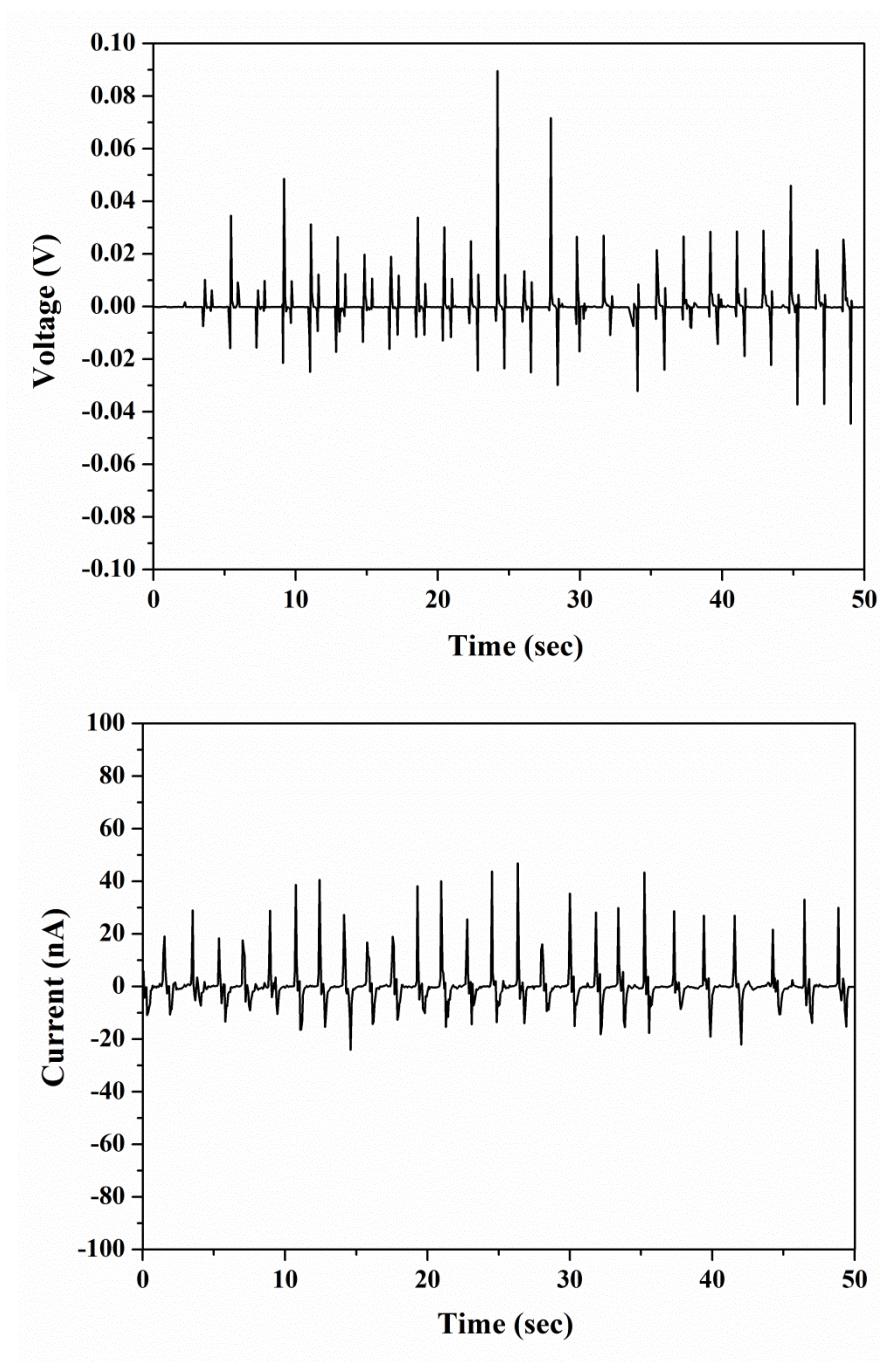


**Figure S12.** (a) Open-circuit voltage and (b) short-circuit current of the PDMS NG measured at a strain and strain rate of 2.1% and 2.2% s<sup>-1</sup>, respectively.

## **VII. Schematic diagram of the ferroelectric domains of KN nanowires**

The spontaneous polarization ( $P_s$ ) direction of the tetragonal perovskite structure is [010].<sup>5</sup> Therefore, when the electric field is applied to the tetragonal KN nanowires during the poling, the domain can rotate 90° (or 180°) both in plane [arrow 1 in Fig. S13(a)] and out of plane [arrow 2 in Fig. S13(a)]. For the orthorhombic perovskite structure, the  $P_s$  direction is [-110].<sup>5</sup> Therefore, the domain in this structure can rotate 90° in plane [arrow 1 in Fig. S13(b)] and 60° (or 120°) out of plane [arrow 2 in Fig. S13(b)] when the electric field is applied. For the PPB structure, in which both tetragonal and orthorhombic structures coexisted,  $P_s$  can rotate 90° in plane [arrow 1 in Fig. S13(c)] and both 90° and 60° (or 120°) along the out of the plane direction [arrows 2 and 3 in Fig. S13(c)]. Therefore,  $P_s$  in the PPB structure can easily rotate and be closely aligned along the applied electric field direction, resulting in the largest piezoelectric strain, thus producing the large output electrical energy.

Figure S14(a) shows a schematic diagram of the ferroelectric domains present in the KN nanowire before the electric poling; the red arrows indicated the direction of  $P_s$ . Since the KN nanowires were randomly distributed in the PDMS, it can be assumed that domains were also randomly distributed in the nanowire without considering the crystal structure of the KN nanowires. When an electric field is applied to the KN nanowire, the domains tend to rotate along the electric field direction. If the KN nanowire has a tetragonal structure, the domains can rotate 90° during poling; the component of the  $P_s$  along the poling direction is indicated by the blue arrow in Figure S14(b). For the orthorhombic KN nanowires, the domain can rotate 90° (in plane) and 60° or 120° (out of plane) during poling; the component of the  $P_s$  along the poling direction is indicated by blue arrows in Figure S14(c). Finally, the domain can rotate 90° in plane and both 90° and 60° (or 120°) along the out of the plane for the PPB KN nanowires; the component of the  $P_s$  along the poling direction is indicated by the blue arrows in Figure S14(d). Furthermore, since the PPB KN nanowires had the largest the  $P_s$  along the poling direction, large output electric energy was obtained from the NG containing the PPB KN nanowires when the strain was applied.

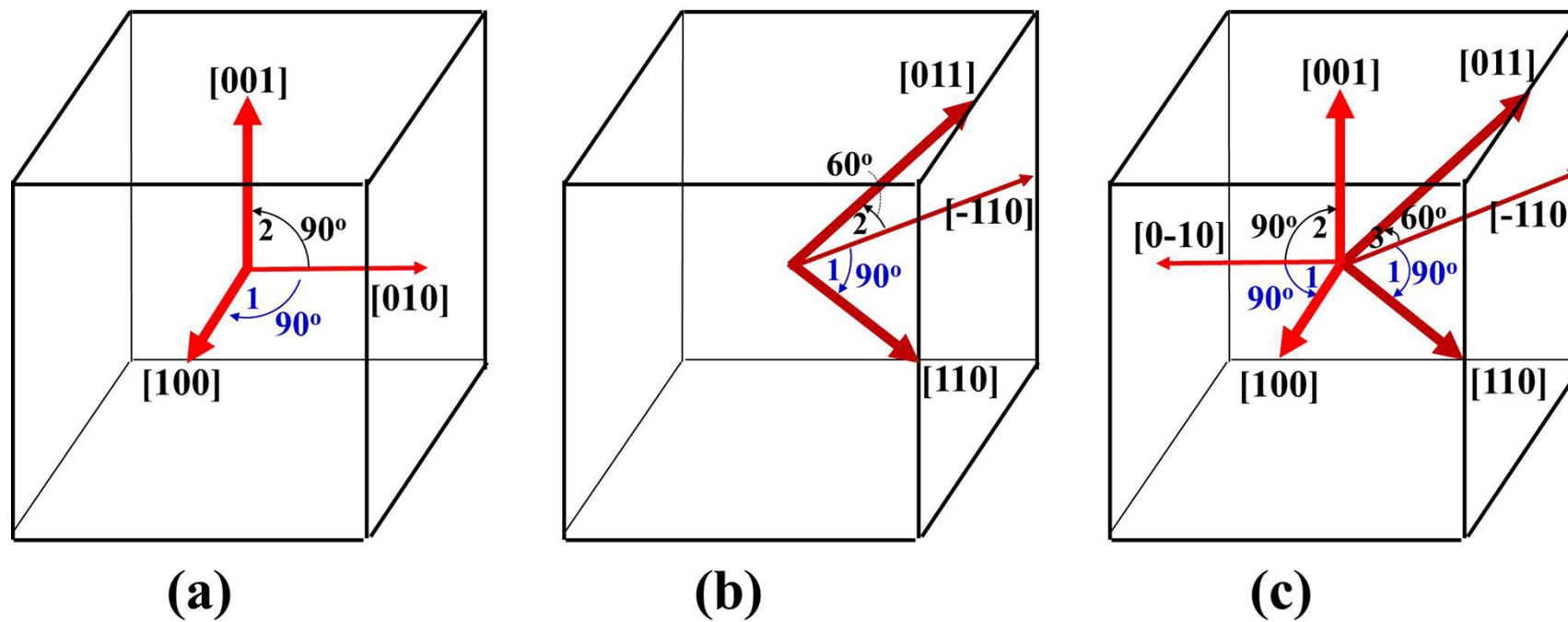


**Figure S13.** Directions of spontaneous polarization in the (a) tetragonal, (b) orthorhombic and (c) PPB structure.

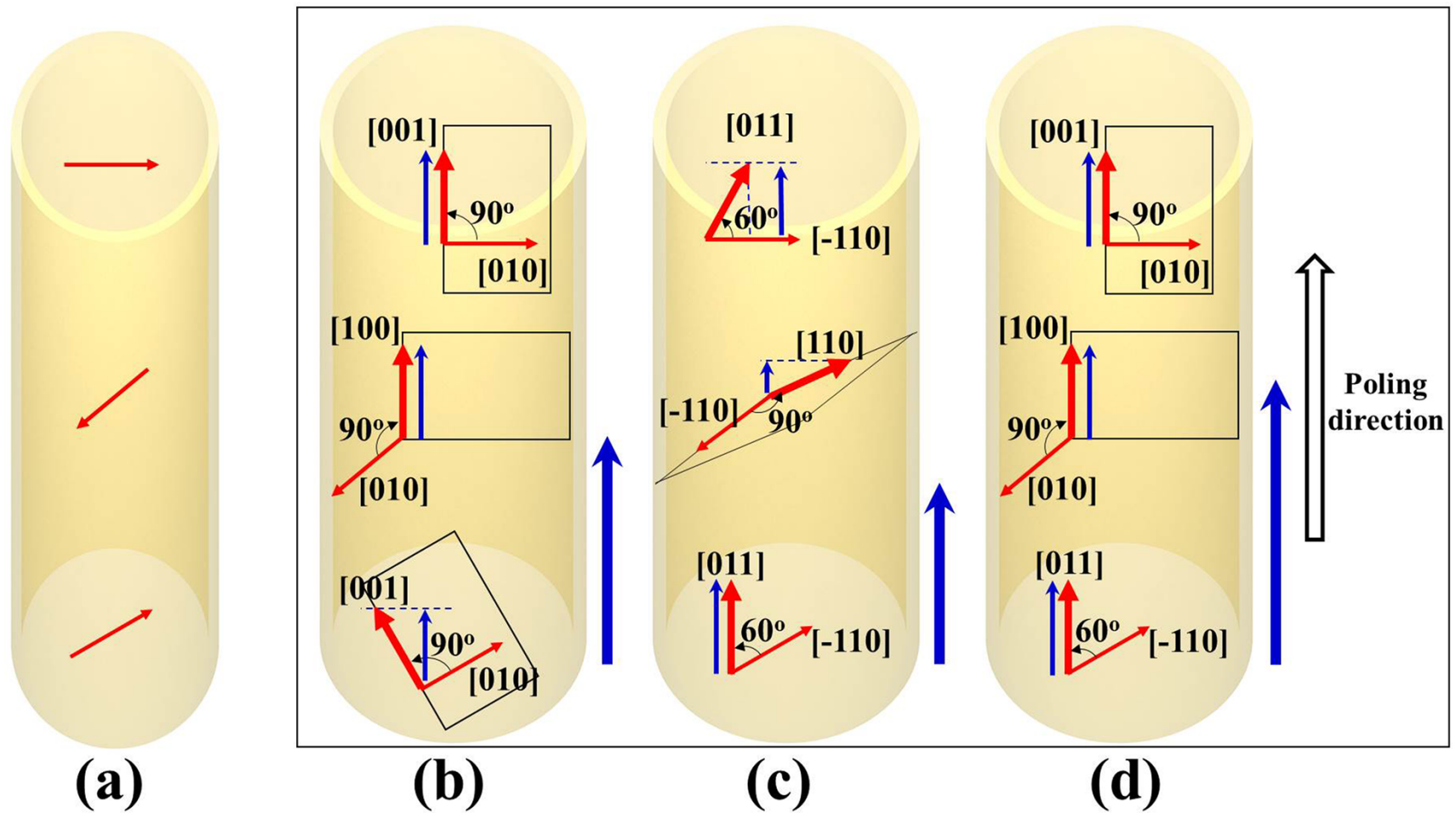


**Figure S14.** Schematic diagram of the ferroelectric domains in the KN nanowires in the PDMS: (a) before the electric poling, (b) tetragonal KN nanowire after poling, (c) orthorhombic KN nanowires after poling, and (d) PPB KN nanowires after poling.

**VIII. Electrical output characteristics of NGs containing various amounts of PPB KN nanowires measured along the reverse direction**

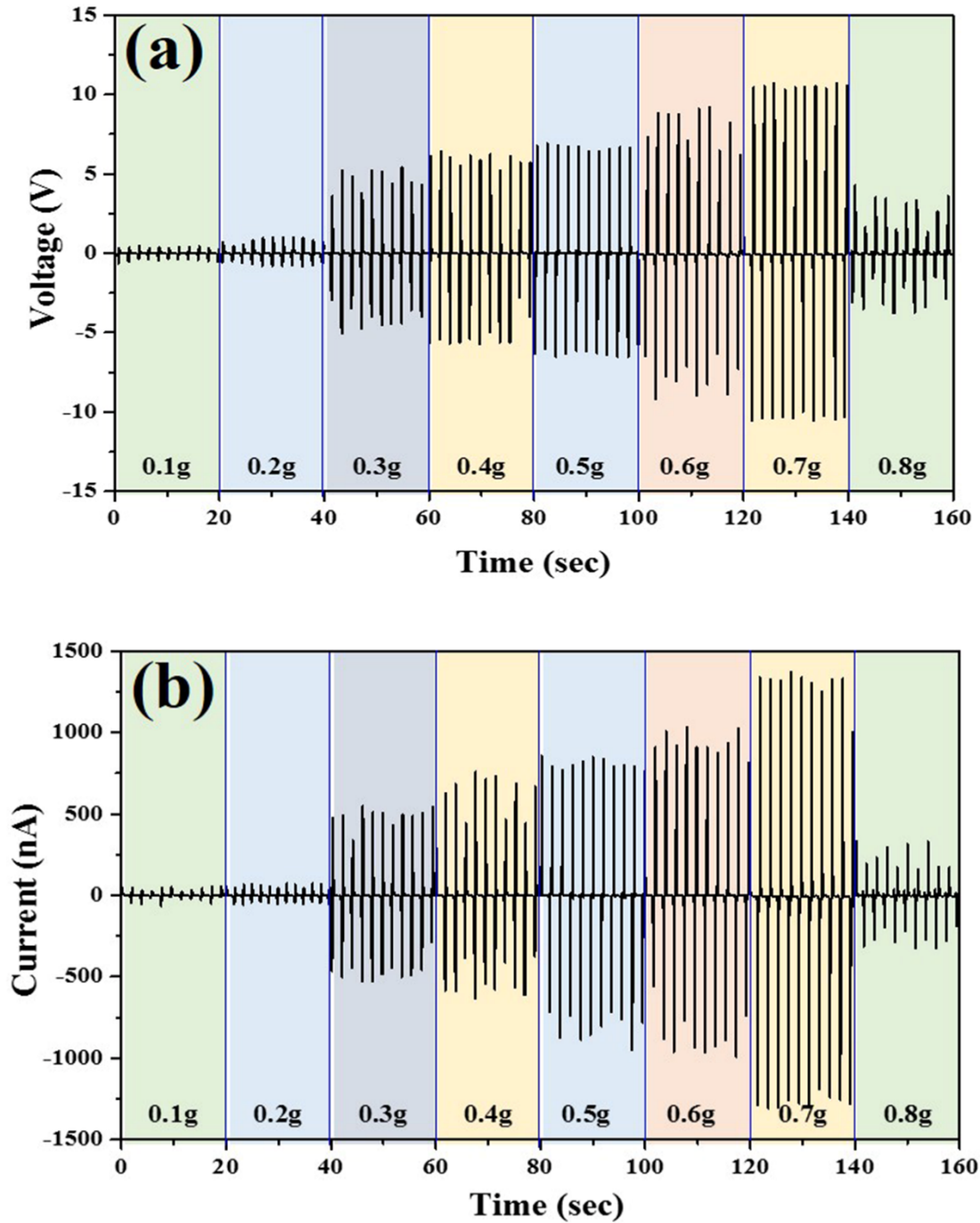


**Figure S15.** (a) Open-circuit output voltage and (b) short-circuit output current of NGs containing various amounts of PPB KN nanowires. The voltage and current were measured along the reverse direction at a strain and strain rate of 2.1% and  $2.2\% \text{ s}^{-1}$ , respectively.

**IX. Electrical output characteristics of NGs measured at various strains and strain rates**

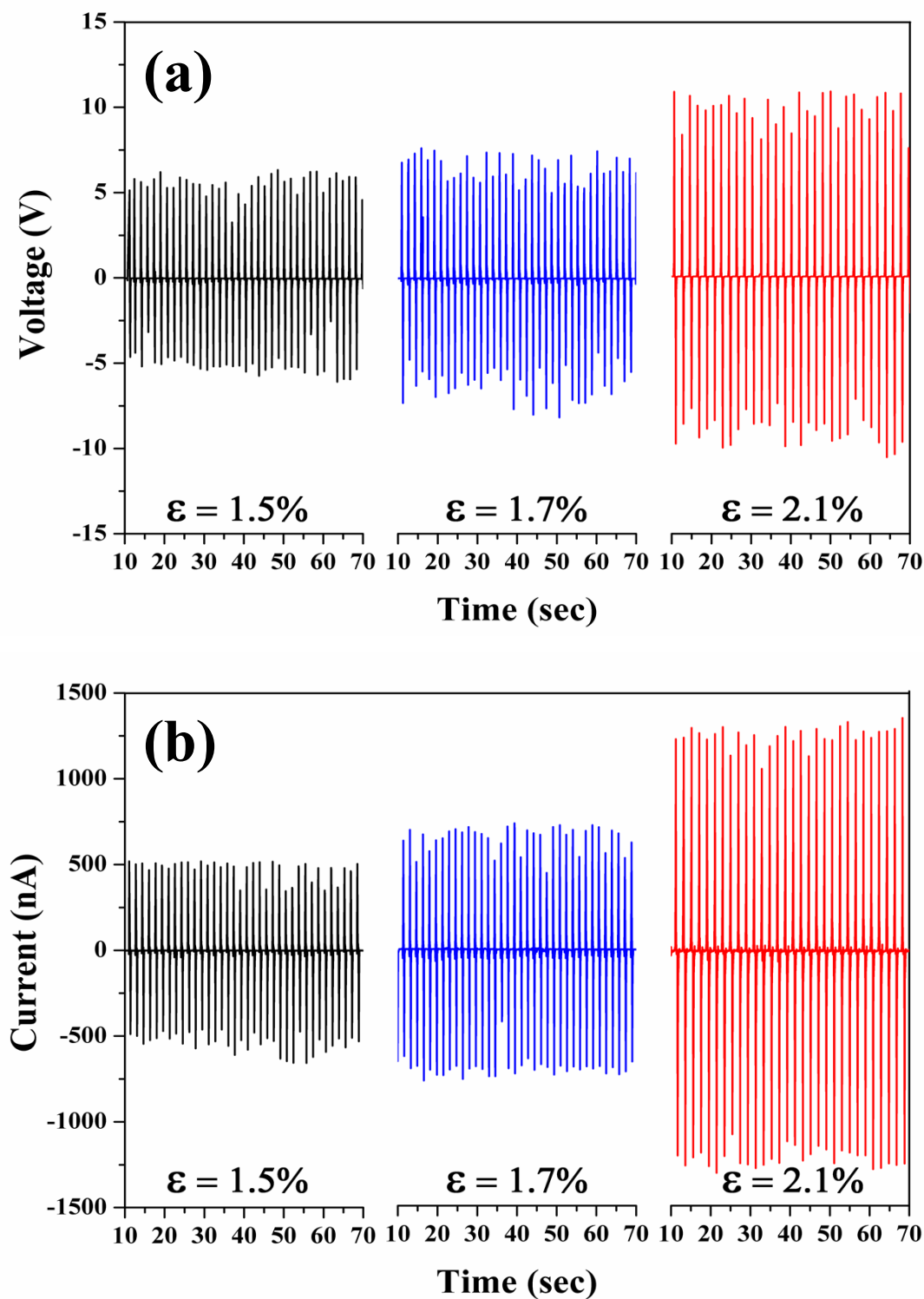


**Figure S16.** (a) Open-circuit output voltage and (b) short-circuit output current of NGs measured at a constant strain rate of  $2.2\% \text{ s}^{-1}$  and various strains.



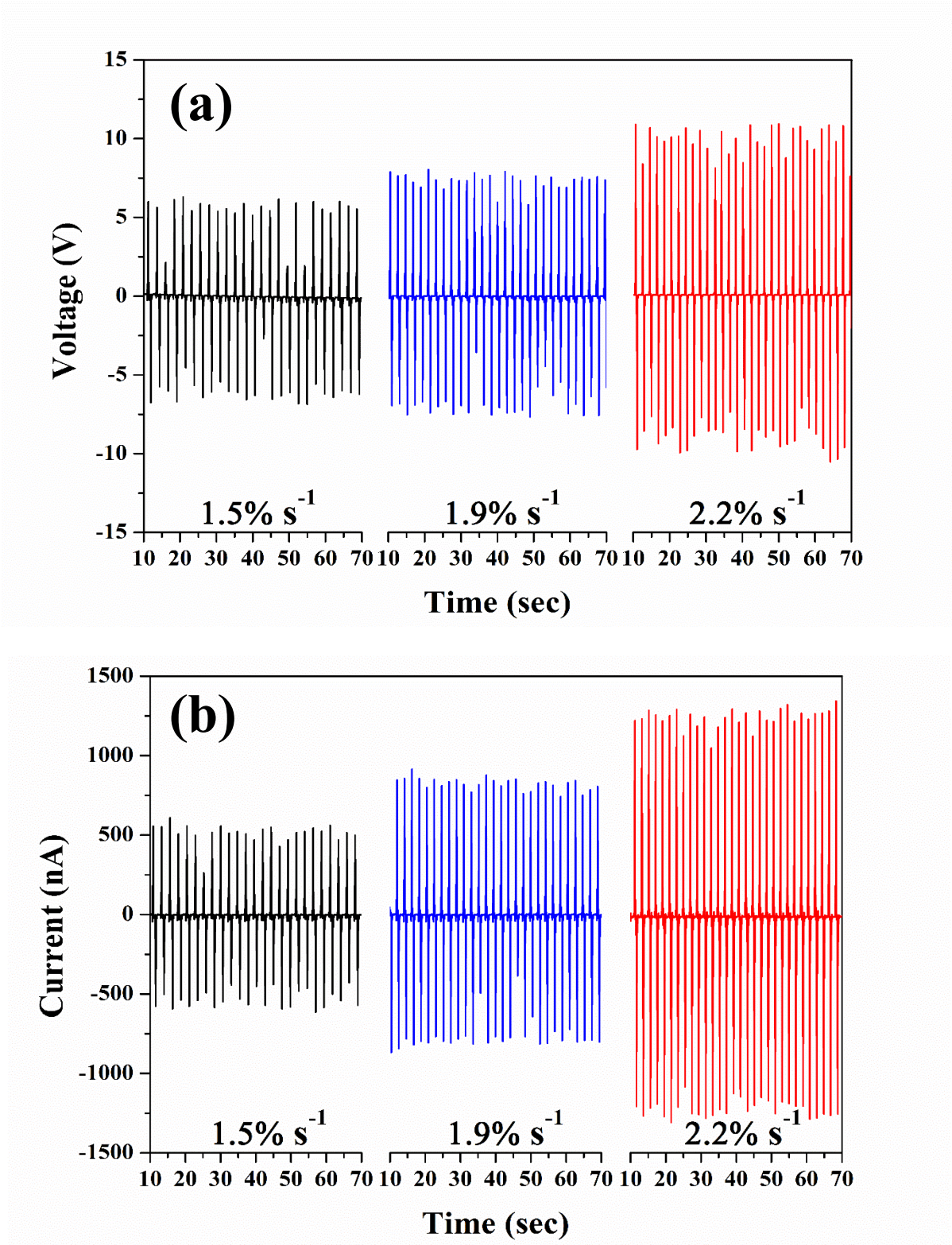


**Figure S17.** (a) Open-circuit output voltage and (b) short-circuit output current of NGs measured at a constant strain of 2.1% and various strain rates.

## References

- <sup>1</sup>J. E. MARK, 'Polymer Data Handbook,' Oxford University Press, Inc., p. 430, 1999.
- <sup>2</sup>J.-H. Jung, C.-Y. Chen, B.-K. Yun, N Lee, Y Zhou, W. Jo, L.-J. Chou, and Z. L. Wang, *Nanotech.* 2012, **23**, 375401.
- <sup>3</sup>R. Yang, Y. Qin, L. Dai, and Z. L. Wang, *Nat. Nanotech.* 2009, **4**, 34.
- <sup>4</sup>C. Chang, V. H. Tran, J. Wang, Y. K. Fuh, and L. Lin, *Nano Lett.* 2010, **10**, 726
- <sup>5</sup>P. Marton, I. Rychetsky, and J. Hlinka, *Phys. Rev. B* 2010, **81**, 144125.